SYNTHESIS AND CHARACTERIZATION OF RESOL TYPE PHENOL-FORMALDEHYDE RESIN IMPROVED BY SIO$_2$-NP

Günay Özbay
Aksaray University
Turkey

Erkan Sami Kokten
Karabuk University
Turkey

Ayhan Ozcifci
Aksaray University
Turkey

ABSTRACT

In this work, resol type phenol–formaldehyde (RPF) resin was modified with silicon dioxide nanoparticles (SiO$_2$-Np). SiO$_2$-Np was added at varying ratios from 1 to 4 wt.% to improve the bonding performance of the RPF resins. The physical characteristics of the nano-modified RPF (nano-RPF) resins were examined. The effects of modification were studied by Fourier transform infrared spectroscopy (FT-IR) and thermogravimetric analysis (TGA). The results of FT-IR revealed that the nano-RPF resins were successfully produced by phenol, formaldehyde, and SiO$_2$-Np. The nano-RPF resins demonstrated high thermal stability at temperatures above 500°C. The adhesive performance of the nano-RPF resins was investigated under dry and wet conditions. The nano-RPF resins indicated better adhesive performance than unmodified RPF resin. The RPF resin could be improved by SiO$_2$-Np.

KEYWORDS: Adhesive performance, phenol–formaldehyde, silica nanoparticles, thermal stability.

INTRODUCTION

Phenol-formaldehyde pre-polymer (PF) resins are the major types of thermosetting polymers, which are widely used as an adhesive by the wood industry is because of its number of

advantages, such as high strength and extremely resistant to moisture of the cured resin (Kariž et al. 2009). PF resins are categorized into two main groups: resols or novolacs depending on the type of catalyst that are used in the production process of the resin. Resol type phenol-formaldehyde resins (RPF) are obtained by the polycondensation reaction of formaldehyde and phenol in a high-alkaline environment. The RPF resins have good thermal, chemical and mechanical properties (Viswanathan and Richardson 1985, Haupt and Sellers 1994, Schmidt 2005, Zhang and Sigman 2007, Riedlinger and Frazier 2008, Moubarik et al. 2009, Roslan et al. 2014, Kurt and Cavus 2011).

There are many studies on PF resin modification by different types of chemicals including boron carbide, boric acid, propylene carbonate, sodium carbonate, and potassium carbonate in order to improve adhesive performance (Gao et al. 1999, Park et al. 1999, Wang et al. 2010). Also, many different types of nano-chemicals such as nano-TiO_2, nano-SiO_2, nano-Fe_2O_3, nano-Al_2O_3, and nano-$CaCO_3$ particles were examined in order to enhance the thermal stability and/or the bond strength of thermosetting adhesives. It was pointed out that the use of nano-chemical could improve the adhesive properties (Cao et al. 2002, Bauer et al. 2006, Li et al. 2007, Shi et al. 2008, Wang et al. 2011). However, there is still a need for experimental studies involving the usage of the nano-chemicals in the polycondensation reaction of the RPF resins production and their applications in the wood products industry.

The purpose of this study is to use silicon dioxide nanoparticles (SiO_2-Np) in the RPF resin synthesis to enhance the adhesive performance of the nano-RPF resins. For this purpose, the effect of SiO_2-Np additives and loading ratio on the chemical and thermal characteristics of the resins were studied by FT-IR and TGA analysis respectively. Then, the bonding performance of laminated wood bonded with the nano-RPF resins was experimentally investigated under indoor/outdoor exposures.

MATERIALS AND METHODS

Materials

Phenol (liquid) and formaldehyde (at a concentration of 37%) were commercial products supplied by GENTAŞ, Turkey. Nano-SiO_2 with the particle size of about 20-30 nm and the density of 0.1-0.15 $g \cdot cm^{-3}$, was supplied by Sigma Aldrich. The beech (*Fagus orientalis* Lipsky) wood planks with a density of 0.670 $g \cdot cm^{-3}$ were used to evaluate the adhesive performance.

Synthesis of the nano-PF resins

The RPF resin syntheses were conducted in a laboratory glass reactor equipped with a condenser, a magnetic stirrer, and a thermometer. The reference resin was based on an unmodified RPF resin (Laboratory made RPF resin). The RPF resin synthesis procedure was as follows: The mixture of phenol and formaldehyde was fed into the reactor and, when the temperature of 60°C was reached, the catalyst, a 2/3 of total NaOH solution (50 wt.%), was added. The mixture was heated to 90°C and, it was followed that the resulting mixtures were heated at 90°C under stirring for 60 min. Then, it was cooled down to a temperature of 60°C. The second part of NaOH (50 wt.%) (1/3 of total NaOH weight solution) was added to adjust the pH to 11.0–12.0 into the reactor at this temperature. At end of the reaction, the mixture was allowed to cool to room temperature. The route for the synthesis of the nano-RPF resins was basically the same as RPF synthesis method. Before the synthesis, various amount of nano-SiO_2 was mixed uniformly with phenol and formaldehyde at room temperature. Loading of the SiO_2-Np in the formulations was variable; 1%, 2%, and 4%.

Characterization

Resol type phenolic resins are generally characterized for final viscosity, pH value, gel time, and solid content. A TES-1380 digital pH meter was employed for pH measurements. Viscosity measurements were carried out at a temperature of 25°C by using a Brookfield viscometer (model: Dv-IPrime). The resin solids content was measured in accordance with ASTM D 3529 (ASTM D3529M-97 2008).

The gel time of the resin was measured at 100°C. The test tube filled with 5 g of prepared the resin was immersed into boiling water and then, constant stirring was applied throughout the test. The elapsed time until the point when no further stirring was possible was defined as the gel time for the sample. The gel time of the resin was determined according to a procedure reported by Haupt and Sellers (1994). Infrared spectra were recorded an Alpha Fourier transform infrared spectrometer. IR spectra were obtained using a frequency range of 4000-400 cm^{-1} with a resolution of 4 cm^{-1} and 40 scans. Thermogravimetric analysis (TGA) was carried out on a HITACHI STA 7300 thermogravimetric analyzer at 5 °C/min under air atmosphere under the nitrogen atmosphere.

Preparation of wood samples and testing

The selected wood lamellas were obtained from beech wood planks with the dimensions of 5 × 50 × 500 mm in the radial, tangential and longitudinal directions, respectively. The lamellas were acclimatized at 20 ± 2°C and 65 ± 3% relative humidity in an acclimatization room. The resin was uniformly applied at the amount of about 180 g·m^{-2} manually by hand brush. Resin was applied on one lamella only. Two wood lamellas bonded with the RFP resin has assembled and hot-pressed under 1.6 MPa pressure at 130°C, for 10 min. The samples were acclimatized in a chamber having 65% relative humidity and temperature of 20°C and then cut into samples with the dimensions of 10 x 20 x 150 mm after the corresponding pre-treatment according to EN 12765 (2002). In bonding tests, 24 samples were evaluated for each group. During the test, the loading was applied centrally and in the plane of the bond. The loading was continued until a break at 2 mm·min^{-1}. The bonding test was performed on a Zwick/Roell Z50 universal testing machine according to BS EN 205 (2003) standard. The following equation was used in order to calculate the tensile shear strength:

$$\sigma_y = F_{max}/A = F_{max}/l_2 \cdot b \tag{1}$$

where: σ_y is the tensile shear strength (N·mm^{-2}), F_{max} is the applied maximum load (N), A is the bonding surface of sample (mm^2), l_2 is the length of the bonded surface (mm), and b is the width of the bonded surface (mm).

RESULTS AND DISCUSSION

Physical characterization

The physical characteristics of the nano-RPF resins are given in Tab. 1. In a comparison of nano-RPF resins with reference resin, the final pH value of the nano-PFR slightly decreases with increasing nano-SiO$_2$ content. As the amount of the nano-SiO$_2$ was increased from 1 wt.% to 4 wt.%, the pH value of the nano-RPF was decreased from 11.84 to 11.62. The decrement of the pH values could be attributed to the low pH value of the nano-SiO$_2$, which is below 3. The viscosity of nano-RPF resins was affected by SiO$_2$-Np content. As the SiO$_2$-Np content

increased, the viscosity values of nano-RPF resins also increased. The lowest viscosity with a value of 285 cPs was measured for the reference RPF resin, while the highest viscosity with a value of 315 cPs was determined for the 4 wt.% SiO_2-Np modified RPF resin. It can be explained that the high molecular weight of the nano-SiO_2 caused an increase in the viscosity of the resin. 4 wt.% SiO_2-Np modified RPF resin had the longest gel time when compared to the reference RPF resin. The solids contents of all the resins including reference RPF and nano-RPF resins were determined to be above 40 wt.%. The SiO_2-Np additive has slightly increased the solids content of the nano-RPF resins. The lowest solid content with a value of 42.84 wt.% was determined for the reference RPF resin, while the highest solid content with a value of 43.51 wt.% was measured for the 4 wt.% SiO_2-Np modified RPF resin (Tab. 1). As reported in the literature, the resin solid content is one of the most important characteristics of phenolic resin. The low solid content adhesive could be ejected out more water during the hot-press processing (Lin et al. 2014).

Tab. 1: Physical characteristics of the nano–PF resins.

Resin type	SiO_2-Np (wt.%)	pH (20°C)	Viscosity (25°C, cPs)	Solid content (%)	Gel time (100°C) (s)
Reference RPF	0	11.98	285	42.84	170
1% SiO_2-Np/RPF	1	11.84	301	43.17	173
2% SiO_2-Np/RPF	2	11.70	309	43.24	176
4% SiO_2-Np/RPF	4	11.62	315	43.51	188

Thermogravimetric analysis

The TGA analysis of the nano-RPF resins was evaluated in a large range of temperatures and it was considered as a measure of the thermal stability. Fig. 1 displays the TGA thermograms of the reference RPF resin and nano-RPF resins. It can be seen that the variations in the thermal stability of the SiO_2-Np modified RPF resin depend upon the temperatures and SiO_2-Np contents. The thermal degradation of these resins can be divided into three regions: 30°C to 120°C, 120°C to 300°C, and 300°C to 600°C. The first region occurred between 30°C and 120°C. This region is probably connected to the removal of the hydroxyl groups. Second region, between 120°C and 300°C, could be related to the terminal weak or strong OH groups. Nano-RPF resins were thermally stable up to 300°C. This thermal stabilization may be explained by new structures, which can be formed during resin synthesis. They are thermally stable until the whole polymer structure collapses (Lin et al. 2006). The weight loss occurs at temperatures between 300°C and 600°C and is caused by oxidative resin degradation. The thermal degradation of the reference RPF resin was higher than the nano-RPF resins. At temperatures below 300°C, nano-RPF resins showed higher thermal stability than reference RPF resin. RPF resin with 2% and 4% SiO_2-Np had higher thermal stability than RPF resin with 1% SiO_2-Np content. At temperatures higher than 300°C, the thermal stability of SiO_2-Np modified RPF resins was higher than that of the reference RPF resin. It can be said that the thermal stability of the RPF resin could be improved by SiO_2-Np. The similar findings, on the thermal stability of phenolic resins, were also reported by Burns and Orrell (1967), Chen et al. (2008), Wang et al. (2011), Bian et al. (2015) as well as Kokten et al. (2020).
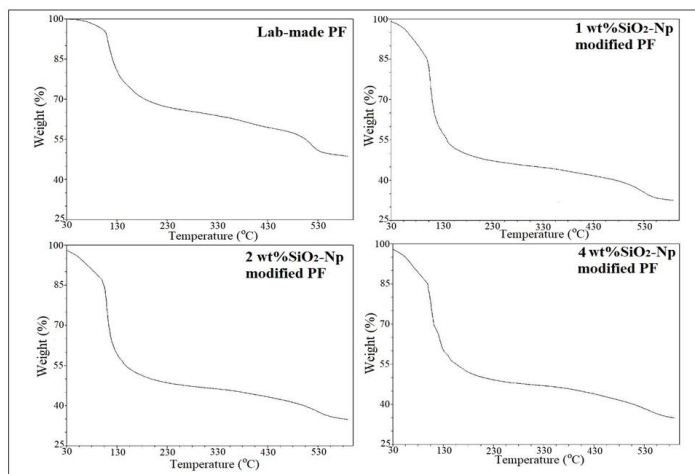
Fig. 1: TGA thermograms of the RPF resins modified by SiO_2-Np.

FT-IR spectroscopy

FT-IR analysis was used to confirm the modification of the RPF and determine the effect of SiO_2-Np on the chemical structure of the RPF resin. The results are shown in Fig. 2. The intense OH stretching band at 3450 cm^{-1} indicated that there are two different types of -OH group: phenolic and alcoholic. The peak shown in the range of 2900–2950 cm^{-1} indicated the symmetrical C-H stretch of CH2. The peaks at around 1700 and 1750 cm^{-1} assigned to the C=C stretching vibrations aromatic ring vibrations group, and also the peak at 1220-1250 cm^{-1} represented the C-O stretching in aromatic ring for all RPF resin. The stretching of C-O-C was found in all RPF resin at 850 cm^{-1}. The characteristic peaks of phenolic compounds were observed at about 1600, 1500, 1450, 1220, and 850 cm^{-1}, as reported in previous FT-IR studies on the PF resin (Liu et al. 2002, Chen et al. 2008, Wang et al. 2009, Zhao et al. 2013, Bobrowski and Grabowska 2015, Cui et al. 2017). New absorptions at 1650 cm^{-1} and 1680 cm^{-1} appeared to compare with the reference RPF resin, the absorptions of the RPF resin containing 4 wt.% SiO_2-Np at 1070–1090 cm^{-1}, representing the dissymmetry flexible vibration of linear Si–O–Si, is more obviously compared to that of the RPF resin containing 1 wt.% SiO_2-Np. The FT-IR results showed that the structures of nano-RPF and the reference RPF resins were similar. This similarity confirmed that nano-RPF resins were successfully synthesized with the SiO_2-Np, phenol, and formaldehyde under the alkali environment.
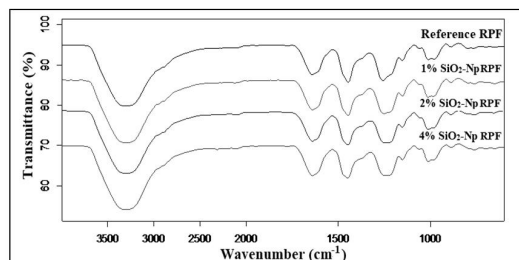

Fig. 2: FT-IR spectra of the nano–RPF resins.

Adhesive performance of the nano-RPF resins

The bond strength values of the specimens are presented in Tab. 2. The highest bond strength with a value of 11.87 $N \cdot mm^{-2}$ was found for the 2 wt.% SiO_2-Np-RPF specimens, followed by 1 wt.% SiO_2-Np-RPF specimens (10.92 $N \cdot mm^{-2}$), reference RPF specimens (10.54 $N \cdot mm^{-2}$), and 4 wt.% SiO_2-Np-RPF specimens (9.76 $N \cdot mm^{-2}$) under dry conditions (pre-treatment 1). The specimens bonded with RPF resins modified by the SiO_2-Np with 1 wt.% and 2 wt.% exceeded standard requirements for the durability of class C1 (10 $N \cdot mm^{-2}$) as defined by EN 12765 (EN 12765 2002). The bond strength values of the resins showed a significant drop under wet conditions, especially pre-treatments 3. The RPF resin containing 2 wt.% SiO_2-Np had the highest strength, while the RPF resin containing 4 wt.% SiO_2-Np reached lower bond strength values after the pre-treatment 2 and pre-treatment 3. However, for the pre-treatment 2 and pre-treatment 3, the RPF resins containing up to 4 wt.% SiO_2-Np satisfy the requirements for durability classes C2 (7 $N \cdot mm^{-2}$) and C3 (4 $N \cdot mm^{-2}$), respectively (Tab. 2). The bond strength test results demonstrated that the bonding performance of the RPF resin could be achieved with SiO_2-Np addition up to 2 wt.% in dry or wet conditions. Many studies stated that silica nanoparticles showed high strength, thermal stability, and chemical stability for polymer materials (Zhou et al. 2003, Sun et al. 2006, Yang et al. 2006, Qin et al. 2017, Zhang et al. 2018).

Tab. 2: The bond strength values of the SiO_2–Np modified RPF resins.

Type of PF resin	Pre-treatment 1 (C1>10)[a]	Pre-treatment 2 (C2>7)[a]	Pre-treatment 3 (C3>4)[a]
Reference RPF	10.54 (0.26)[b]	7.38 (0.21)	5.69 (0.39)
1% SiO_2-Np/RPF	10.92 (0.32)	7.44 (0.34)	6.03 (0.43)
2% SiO_2-Np/RPF	11.87 (0.48)	7.59 (0.31)	6.14 (0.35)
4% SiO_2-Np/RPF	9.76 (0.32)	6.58 (0.45)	5.27 (0.41)

[a]Minimum requirements of adhesive bond strength in $N \cdot mm^{-2}$ according to EN 12765 for each pre-treatment.
[b]The values in the parentheses are standard deviations.

CONCLUSIONS

The purpose of this study is to show usability of silicon dioxide nanoparticles (SiO_2-Np) in the RPF resin synthesis to enhance the adhesive performance of the nano-RPF resins. The effect of SiO_2-Np contains on the physical, chemical, and thermal characteristics of the resins were examined. The following conclusions can be outlined:

- The physical characteristics such as pH, viscosity, solid content and gel time of the nano-RPF resin were affected by SiO_2-Np content.
- The RPF resins modified by SiO_2-Np showed higher thermal stability than the reference RPF resin. The RPF resin with 2% and 4% SiO_2-Np had higher thermal stability than RPF resin with 1% SiO_2-Np content. The thermal stability of the RPF resin could be improved by SiO_2-Np.
- The results of the FT-IR spectrum showed that the nano-RPF had a similar FT-IR spectrum to the reference RPF resin. The molecular structure relationship demonstrated that nano-RPF resins were successfully synthesized with the SiO_2-Np, phenol, and formaldehyde under the alkali environment.
- The adhesive performance test results revealed that the bond strength of the RPF resin could be improved with SiO_2-Np addition up to 2 wt.%. Nano-based resins can be used in the production of wood adhesives.

ACKNOWLEDGMENTS

REFERENCES

1. ASTM D3529M-97, 2008: Standard test method for matrix solids content and matrix content of composite prepreg.

2. Bauer, F., Decker, U., Ernst, H., Findeisen, M., Langguth, H., Mehnert, R., Sauerland, V., Hinterwaldner, R., 2006: Functionalized inorganic/organic nanocomposites as new basic raw materials for adhesives and sealants. Part 2. International Journal of Adhesion and Adhesives 26(7): 567-570.

3. Bian, C., Wang, Y., Wang, S., Zhong, Y., Liu, Y., Jing, X., 2015: Influence of borate structure on the thermal stability of boron-containing phenolic resins: A DFT study. Polymer Degradation and Stability 119: 190–197.

4. Bobrowski, A., Grabowska, B., 2015: FTIR method in studies of the resol type phenol resin structure in the air atmosphere in some time intervals. Metallurgy and Foundry Engineering 41(3): 107.

5. BS EN 205, 2003: Adhesives. Wood adhesives for non-structural applications. Determination of tensile shear strength of lap joints.

6. Burns, R., Orrell, E.W., 1967: A thermal analytical study of phenol formaldehyde resins. Journal of Materials Science 2(1): 72-77.

7. Cao, Y.M., Sun, J., Yu, D.H., 2002: Preparation and properties of nano-Al_2O_3 particles/polyester/epoxy resin ternary composites. Journal of Applied Polymer Science 83(1): 70-77.

8. Chen, Y., Chen, Z., Xiao, S., Liu, H., 2008: A novel thermal degradation mechanism of phenol–formaldehyde type resins. Thermochimica Acta 476(1): 39-43.

9. Cui, Y., Hou, X., Wang, W., Chang, J., 2017: Synthesis and characterization of bio-oil phenol formaldehyde resin used to fabricate phenolic based materials. Materials (Basel), 10(6): 668.

10. EN 12765, 2002: Classification of thermosetting wood adhesives for non-structural applications.

11. Gao, J., Liu, Y., Yang, L., 1999: Thermal stability of boron-containing phenol formaldehyde resin. Polymer Degradation and Stability 63(1): 19-22.

12. Haupt, R.A., Sellers, T.J., 1994: Characterizations of phenol-formaldehyde resol resins. Industrial & Engineering Chemistry Research 33(3): 693-697.

13. Kariž, M., Jošt, M., Sernek, M., 2009: Curing of phenol-formaldehyde adhesive in boards of different thicknesses. Wood Research 54(2): 41-48.

14. Kokten, E.S., Özbay, G., Ayrilmis, N., 2020: Synthesis of biobased phenolic resins using catalytic pyrolysis oil and its effect on oriented strand board performance. The Journal of Adhesion 96(5): 475-489.

15. Kurt, R., Cavus, V., 2011: Manufacturing of parallel strand lumber (PSL) from rotary peeled hybrid poplar I-214 veneers with phenol formaldehyde and urea formaldehyde adhesives. Wood Research 56(1): 137-144.

16. Li, H., Zhang, Z., Ma, X., Hu, M., Wang, X., Fan, P., 2007: Synthesis and characterization of epoxy resin modified with nano-SiO$_2$ and γ-glycidoxypropyltrimethoxy silane. Surface and Coatings Technology 201(9-11): 5269–5272.

17. Lin, R., Fang, L., Li, X., Xi, Y., Zhang, S., Sun, P., 2006: Study on phenolic resins modified by copper nanoparticles. Polymer Journal 38(2): 178.

18. Lin, R., Sun, J., Yue, C., Wang, X., Tu, D., Gao, Z., 2014: Study on preparation and properties of phenol-formaldehyde-chinese fir liquefaction copolymer resin. Maderas Ciencia y Tecnologia 16(2): 159–174.

19. Liu, Y., Gao, J., Zhang, R., 2002: Thermal properties and stability of boron-containing phenol-formaldehyde resin formed from paraformaldehyde. Polymer Degradation and Stability 77(3): 495–501.

20. Moubarik, A., Pizzi, A., Allal, A., Charrier, F., Charrier, B., 2009: Cornstarch and tannin in phenol–formaldehyde resins for plywood production. Industrial Crops and Products 30(2): 188–193.

21. Park, B.D., Riedl, B., Hsu, E.W., Shields, J., 1999: Differential scanning calorimetry of phenol–formaldehyde resins cure-accelerated by carbonates. Polymer 40(7): 1689-1699.

22. Qin, W., Vautard, F., Askeland, P., Yu, J., Drzal, L.T., 2017: Incorporation of silicon dioxide nanoparticles at the carbon fiber-epoxy matrix interphase and its effect on composite mechanical properties. Polymer Composites 38(7): 1474–1482.

23. Riedlinger, D.A., Frazier, C.E., 2008: Morphological analysis of PF/pMDI hybrid wood adhesives. Journal of Adhesion Science and Technology 22(12): 1197–1208.

24. Roslan, R., Zakaria, S., Chia, C.H., Boehm, R., Laborie, M.P., 2014: Physico-mechanical properties of resol phenolic adhesives derived from liquefaction of oil palm empty fruit bunch fibres. Industrial Crops and Products 62: 119–124.

25. Schmidt, R.J., 2005: Industrial catalytic processes - phenol production. Applied Catalysis A: General 280(1): 89–103.

26. Shi, H., Liu, F., Yang, L., Han, E., 2008: Characterization of protective performance of epoxy reinforced with nanometer-sized TiO$_2$ and SiO$_2$. Progress in Organic Coatings 62(4): 359–368.

27. Sun, S., Li, C., Zhang, L., Du, H.L., Burnell-Gray, J.S., 2006: Effects of surface modification of fumed silica on interfacial structures and mechanical properties of poly (vinyl chloride) composites. European Polymer Journal 42(7): 1643-1652.

28. Viswanathan, T., Richardson, T., 1985: Thermosetting adhesive resins. Patent US4524164A.

29. Wang, J., Jiang, N., Jiang, H., 2010: Micro-structural evolution of phenol-formaldehyde resin modified by boron carbide at elevated temperatures. Materials Chemistry and Physics 120(1): 187–192.

30. Wang, M., Leitch, M., Xu, C.C., 2009: Synthesis of phenol–formaldehyde resol resins using organosolv pine lignins. European Polymer Journal 45(12): 3380–3388.

31. Wang, Z., Gu, Z., Hong, Y., Cheng, L., Li, Z., 2011: Bonding strength and water resistance of starch-based wood adhesive improved by silica nanoparticles. Carbohydrate Polymers 86(1): 72–76.

32. Yang, H., Zhang, Q., Guo, M., Wang, C., Du, R., Fu, Q., 2006: Study on the phase structures and toughening mechanism in PP/EPDM/SiO$_2$ ternary composites. Polymer 47(6): 2106-2115.

33. Zhang, Y., Sigman, M.S., 2007: Palladium (II)-catalyzed enantioselective aerobic dialkoxylation of 2-propenyl phenols: A pronounced effect of copper additives on enantioselectivity. Journal of the American Chemical Society 129(11): 3076-3077.

34. Zhang, Z., He, X., Wang, X., Rodrigues, A.M., Zhang, R., 2018: Reinforcement of the mechanical properties in nitrile rubber by adding graphene oxide/silicon dioxide hybrid nanoparticles. Journal of Applied Polymer Science 135(14): 46091.

35. Zhao, Y., Yan, N., Feng, M.W., 2013: Thermal degradation characteristics of phenol–formaldehyde resins derived from beetle infested pine barks. Thermochimica Acta 555: 46-52.

36. Zhou, S., Wu, L., Sun, J., Shen, W., 2003: Effect of nanosilica on the properties of polyester-based polyurethane. Journal of Applied Polymer Science 88(1): 189–193.

Günay Özbay
Aksaray University
Department of Industrial Engineering
68100 Aksaray
Turkey

Erkan Sami Kokten*
Karabuk University
Department of Industrial Engineering
78050 Karabuk
Turkey
*Corresponding author: erkansamikokten@karabuk.edu.tr

Ayhan Ozcifci
Aksaray University
Department of Industrial Engineering
68100 Aksaray
Turkey